Hydrophobic Treatment of Woven Cotton Fabrics with Polyurethane Modified Aminosilicone Emulsions

Giulia Mazzon[a,b], Muhammad Zahid[a], Jose A. Heredia-Guerrero[a], Eleonora Balliana[b], Elisabetta Zendri[b], Athanassia Athanassiou[a,*], Ilker S. Bayer[a,*]

[a]*Smart Materials group, Istituto Italiano di Tecnologia, via Morego, 30 -16163 Genova, Italy.*
[b]*Dipartimento di Scienze Ambientali, Informatica e Statistica, Università Ca' Foscari di Venezia, via Torino 155, Mestre Venezia, Italy.*

ABSTRACT

Woven cotton fabrics were treated with a polyurethane modified aminosilicone fluid commonly used as a fabric softener. The aminoethylaminopropyl polydimethylsiloxane was modified with an aqueous dispersion of polycarbonate diol polyurethane using isopropyl alcohol as co-solvent resulting in stable micro-emulsions with an average droplet size of 1.5 μm. Polycarbonate polyurethane was chosen due to its good hydrolytic stability and low water absorption levels. Fabrics were treated either by immersion in emulsions or by spray coating. Treated fabrics had static water contact angles exceeding 143^{o} with droplet shedding angles of less than 50^{o} depending on the droplet volume. Treated textiles were breathable with vapor permeability levels of 5.6 mg (m day Pa)$^{-1}$ that was similar to untreated fabrics. Good droplet shedding action was achieved based on the inherent fiber roughness. Accelerated ageing tests corresponding to 5 years using CIEL*a*b standards (7.5×10^{6} lux·hours exposure) indicated that no ageing occurred, with the overall color parameter of $\Delta E<2.0$ indicating invisible color changes to the naked eye. This sustainable approach can be easily scaled and may be a valuable treatment alternative for delicate fabrics commonly encountered in Heritage preservation; but also for many other cotton-based textiles.

E-mails: ilker.bayer@iit.it (I. S. Bayer); athanassia.athanassiou@iit.it (A. Athanassiou)

Key words: cotton fabric, modified aminosilicone, application method, self-cleaning, hydrophobic performance

1. INTRODUCTION

Hydrophobic and liquid-repellent textiles have been extensively studied in the last decades to render them functional in applications such as oil-water separation [1], [2], [3] self-cleaning fabrics [4], [5], [6], breathable and water repellent clothes [7], [8], [9]. Related treatments can protect textiles, and enhance their lifetime by preventing water absorption-related degradation of fibres [10], [11], [12] and by improving the fibres' strength [13]. Many efficient surface treatments have appeared on textiles in the last decade and more and more sustainable and eco-friendly approaches have also been reported latterly [13], [14], [15]. Although highly effective towards repelling low surface tension liquids [16], [17], [18], [19], [20], one of the issues related to fluorinated treatments is the use of C-8 fluorinated compounds like C-8 co-polymers, fluorinated-silanes or monomers that are known to break down into persistent perfluorooctanoic acid (PFOA) and perfluorooctanesulfonate (PFOS) [21]. Hence, the Environmental Protection Agency (EPA) prohibited C-8 fluoropolymer and related chemicals production starting from 2015 [22]. Due to this, short-chain fluorinated homologues such as C6 fluorochemicals/polymers have been implemented instead. Although it is demonstrated that the toxicity of the perfluoroalkyl compounds decreases with decreasing carbon chain length [23], their hydrophobic performance and durability are also compromised [24].

Polydimethylsiloxane (PDMS) polymers, also known as silicones, are highly popular compounds that are biocompatible [25], [26] with good hydrophobic properties. They are generally dissolved in organic solvents [27], [28], [29], [30]. However, solvent-based treatments are generally challenging for scale up in industry. Therefore, some silicones have been commercialized as water dispersions or as low viscosity functional polysiloxanes [31] for textile use but particularly as softeners rather than for waterproofing. Silicone emulsions with or without other polymers in water can be highly promising vehicles to produce water repellent textiles [11], [32]. In order to disperse polysiloxane polymers in water, the silicone chains are modified by hydrophilic polar and reactive moieties (end-groups) such as amino-silicones [33] and phenyl-carboxyl-polydimethylsiloxanes [34] that are developed for water emulsions. Although much less

hydrophobic compared to silicone [35], waterborne polyurethanes are commonly applied on textiles because of their breathability [36] toughness, abrasion resistance [37], excellent adhesion to surface [38] and flexibility [39].

In this work, we emulsified an aminoethylaminopropyl polydimethylsiloxane fluid [40], [41], [42] with a waterborne polyurethane dispersion to produce a permanent hydrophobic cotton fabric formulation. Simple dip or spray coating can be used to transform the fabric. Coatings were applied so that formation of laminating layers over the fabric was avoided. Intrinsic roughness of the fibres helped attaining high water contact angles and water droplet mobility. The wetting properties of the treated cotton fabrics were tested as well as their mechanical properties vapour permeability, colour variation, and resistance to ageing. The results indicated that the treated cotton textiles remain hydrophobic with water droplet shedding ability, even though they did not comply with the generally accepted superhydrophobicity criteria, specifically, contact angles above 150^{o} and roll-off angles below 5^{o}. The developed formulation may be used in the treatment of historical textiles conserved in museums or indoor environments in addition to highly hydrophobic textiles for garments or sportswear.

2. MATERIALS AND METHODS

2.1 Materials

The textile used was a plain woven and bleached 100% cotton fabric, with 180 ± 5 g/m^2 mass density and having 24 threads/cm density in each direction. A solvent-free, waterborne dispersion of an aliphatic polyurethane based on polycarbonate diols [43], [44] named ESACOTE PU 77 (hereafter, PCU) was supplied by Lamberti S.p.A. (Italy). An aminosilicone fluid (aminoethylaminopropyl silicone) named FINISH WR 1300 was purchased from WACKER® (Germany). The silicone fluid contains more than 85 wt.% 3-((2-aminoethyl)amino)propyl)methyl(dimethyl) siloxane, methoxy-terminated (as IUPAC name), and the rest 15 wt.% is made up of octamethyl cyclotetrasiloxane and trace amounts of ethanol.

2.2 Preparation and characterization of polymer dispersions

The solids content of the as-received waterborne PCU was measured to be 36 wt. % after drying a film cast on a glass slide under laboratory conditions (~20^{o}C). The commercial PCU solution was diluted by adding water so that a 2 wt.% final solution is obtained. Similarly, the commercial silicone fluid was dispersed in isopropyl alcohol (IPA) to obtain a 2 wt. % solution. Afterwards, 40 mL of each diluted solution were combined in a different vial and upon gentle mechanical mixing a homogeneous polyurethane/silicone dispersion was obtained. The obtained dispersion was stable for long periods (weeks) with no phase separation. **Figure 1(a)** shows photographs of 2 wt.% PCU (in water) and aminosilicone (in IPA) dispersions along with their blend that assumes a milky emulsion state.

Droplet distribution in each 2 wt. % dispersion including the blend was analyzed by Dynamic Light Scattering (DLS) and the results are shown in **Fig. 1(b)**. Aminosilicone fluid has the smallest average droplet size of 5 nm, whereas the PCU dispersion average droplet size is about 30 nm, indicating that both diluted dispersions are polymeric nano-suspensions. Upon blending, however, the average dispersion droplet size increases to 1.5 μm but nonetheless the dispersion remains highly stable.

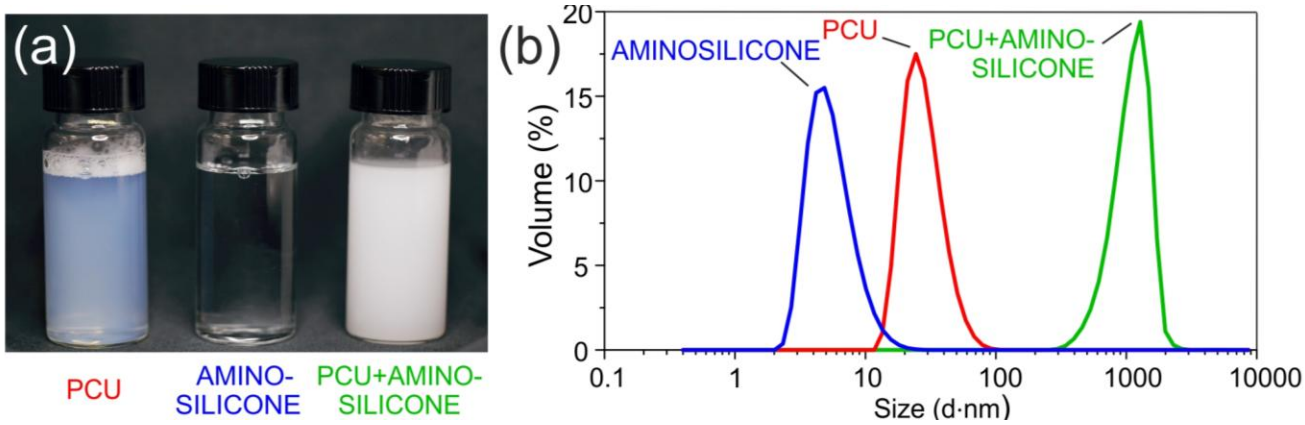

Figure 1. (a) Photograph of commercial PCU (hazy white) and the aminosilicone (transparent) dispersions and the emulsion (white), (b) DLS analysis indicate droplet size distribution of the commercial dispersions and the emulsion.

2.3 Details of fabric treatment and sample preparation

The cotton fabric was washed and dried before use to ensure a contamination free fabric. The fabric was cut into pieces of (10 × 15) cm^2 size before applying the treatments. Single polymer treatments, namely, only PCU and only silicone (softener) were also made as control samples. Following this, sequential polymer treatments (i.e., double layer) were also made. Specifically, first the PCU treatment solution was applied and after drying and curing at 60 °C for 24 hours, the aminosilicone layer solution was applied followed by the same drying and curing process. Before characterization of the treated textiles, the samples were stored at room temperature (20°C and ~ 40% RH) for another 24 hours. Fabrics were treated either with spray (Paasche Airbrush VL with 73 mm head and 1.06 mm tip) or dip coating in order to find the optimum application method.

Spray application was performed by spraying a total of 40 mL of the dispersions on both sides of the textile's pieces. It was important to spray both sides to obtain a symmetric hydrophobic behavior [4]. Spraying distance was maintained approximately at 20 cm for the aminosilicone dispersion in IPA, at 40 cm for PCU dispersion in water and at approximately 30 cm for the PCU/Aminosilicone polymer blend dispersion. Dip-coating was performed by immersing each sample in the specific solution for 15 s in order to guarantee efficient absorption of the product in the textile. Table 1 lists the type of samples prepared for further characterization and analysis. In short, S1 is the untreated woven cotton textile, double layer refers to the sequential application of PCU and aminosilicone solutions, whereas micro-emulsion refers to single step application of the emulsions.

Table 1. Description of samples produced, treatments and application methods.

Sample name	Treatment			Application method	
	untreated	double-layer	micro-emulsion	dip	spray
S1	✓				
S2		✓		✓	
S3			✓	✓	
S4		✓			✓
S5			✓		✓

2.4 Characterization

2.4.1 Morphological characterization

Scanning electron microscopy (SEM) and Atomic force microscopy (AFM) were used to analyze the micro-morphology of the samples and their fiber surfaces. SEM images were acquired using a JEOL JSM-6490LA (Japan), operating at 10 kV acceleration voltage. Prior to imaging, the samples' surfaces were sputtered with a 10 nm thick film of gold (Cressington 208HR sputter coater, UK). SEM images were collected at different magnifications such as 25X, 50X, 1000X. In addition, elemental analysis and mapping by energy-dispersive x-ray spectroscopy (EDX) were performed to confirm coating homogeneity.

AFM measurements were carried out with XE-100 instrument (Park Systems, Korea) maintained on an anti-vibration platform TS-150 (Table Stable, Switzerland) and used in non-contact mode. Non-Contact Cantilever probes (Park, Korea) were used, with nominal resonance frequency of 330 kHz. The scan rate was 0.1 Hz and the scan area was 2x2 μm^2. The acquired images were processed with WSxM 5.0 software and the roughness characteristics of the surfaces were determined by using Gwyddion software, which gave root mean square roughness (Sq) and average roughness (Sa). Final results are the averages obtained by 4 to 6 different samples measurements, with the standard deviation reported as the uncertainty [45], [46].

2.4.2 Attenuated Total Reflection-Fourier Transform Infrared (ATR-FTIR) spectroscopy

Infrared spectra were acquired by a single-reflection attenuated total reflection (ATR) accessory (MIRacle ATR, PIKE Technologies), with a diamond crystal coupled to a Fourier Transform Infrared (FTIR) spectrometer (Equinox 70 FT-IR, Bruker). All spectra were recorded in the range from 3800 to 600 cm^{-1} with a resolution of 4 cm^{-1}, accumulating 128 scans. Three analyses were performed for each sample to ensure the reproducibility of obtained spectra.

2.4.3 Wettability measurements and surface energy estimation

In order to study the surface wettability of the fabrics, static water contact angles (WCA) and water shedding angle (WSA) or droplet roll-off angle were measured with a contact angle instrument (OCAH-200 DataPhysics, Germany) at room temperature (~23 °C). As for WCA, a gas-tight 500 mL Hamilton precision syringe with blunt needle of 0.52 mm internal diameter was used to deposit milli-Q water droplets of 5 µL. WCAs were automatically calculated by the software based on the droplet shape. Ten droplets were deposited on each sample in different positions and then the averages were calculated [47]. With the same instrument, the roll-off angle analyses were carried out. Droplets of 17.5µL, 20 µL, 25 µL, 30 µL and 35 µL were deposited on the surface, which was then inclined at an angular speed of 1.42^{o}/s. Side view images of the drops were captured and the roll-off angle was recorded. Measurements were repeated 5 times. [27].

Water droplet wetting and penetration into the fabrics were separately tested by using larger water colored droplets in order to assess long term wetting stability. 0.1 wt.% of food colorant (Color Dolci F.lli Rebecchi Valtrebbia S.p.A) was added to water and then 1 mL droplet was deposited on the surface of the tested fabric. The droplet was monitored until it was completely absorbed or evaporated depending on the hydrophobicity of the fabric. Residual color stains allowed assessment of fabric performance against wetting by heaver drops over longer periods. Furthermore, the surface energy of the hydrophobic PCU/silicone composite treatment on the fabrics was estimated using the critical surface tension (γ) concept of Zisman plot [48]. A series of contact angles were measured on the hydrophobic fabrics using the following liquids: water, glycerol, dimethylformamide, toluene, isopropyl alcohol and n-hexane. Their surface tensions were then plotted against the cosine value of the corresponding static contact angles. The best fit of the points was extrapolated. From this fit, at the intersection with the value of $\cos\theta = 1$, on horizontal axis the value of γ was obtained.

2.4.4 Water vapor permeability

Water vapor permeability (WVP) of the untreated and treated fabrics was determined at 25°C and under 100% relative humidity gradient ΔRH (%) according to the ASTM E96 standard method. Humidity gradient (ΔRH) was accomplished by placing 400 µL of deionized water in

the permeation chambers of 7 mm inner diameter and 10 mm height. Properly sized samples were cut and mounted on the top of the permeation chamber and sealed. The chambers were placed in a desiccator, maintained at 0% RH by anhydrous silica gel. The weight changes of the chambers were registered every hour for 8 consecutive hours, in order to monitor the transfer of water from the chamber, through the sample, to the desiccant. An electronic balance (with 0.0001 g accuracy) was used to record mass loss over the time. The water mass loss of permeation chambers was plotted as a function time. The slope of each line was calculated by linear regression. Then, the water vapor transmission rate (WVTR) was determined as below:

$$WVTR(g(m^2d)^{-1}) = \frac{slope}{area\ of\ the\ sample}$$

The water vapor permeability (WVP) of the samples was calculated as follows:

$$WVP(g(mdPa)^{-1}) = \frac{WVTR \cdot L \cdot 100}{p_S \cdot \Delta RH}$$

where L(m) is the thickness of the sample, which was measured with a micrometer with 0.001mm accuracy, ΔRH (%) is the percentage relative humidity gradient, and p_s (Pa) is the saturation water vapor pressure at 25°C [6], [49], [50]. Every measurement was replicated three times.

2.4.5 Stress-strain measurements

Mechanical characterization of the fabrics was obtained with 3365 Instron (USA) tensile tester. Prior to testing, the samples were conditioned at room temperature. Specimens were cut with a dog shaped mechanical cutter, giving them the standard dimension of 25 mm length along the axis of warp threads and 3.98 mm width. Samples were placed in between pneumatic clamps and a constant rate of extension of 5 mm/min was applied. The elastic modulus (MPa) was calculated using the initial slope of the curve, between 0 and 0.1 mm/mm. Elongation at maximum load values was also calculated. The average elastic moduli and elongation values of 5 measurements with standard deviations are reported [51], [52].

2.4.6 Flexural rigidity

Changes in tactile properties of textile fabrics are strongly dependent on various structural, mechanical, and surface parameters [51], [53], [54]. The bending properties and the drapability (degree to which a fabric can be draped) cannot be determined from in-plane properties and a separate test is required. Hence, the flexural rigidity was determined with the cantilever test [55]. The samples were first tested in a standard cantilever test device equipped with a level and an etched line inclined at 41.5° on one face of the set-up. Fabrics were cut in dimensions of 200mm × 25mm, placed on the smooth horizontal platform with a weighed slide on it and gradually slid over the edge at constant speed, until the leading edge of the fabric made contact with the banding angle (41.5°) indicator of the device. The flexural rigidity G_{Pierce} (Nm) was calculated according to the formula [55]:

$$G_{Pierce} = 9.81 \cdot 10^{-12} \cdot w \cdot c^3$$

where w (g/m^2) is the weight of each coated sample and c (mm) is the bending length measured during the cantilever test. Stiffness is given here in sense of bending length of the fabric. A higher value of the bending length indicates higher fabric stiffness [46]. For each sample, the face and back of both extremities were tested, leading to a total of four measurements per sample [55].

2.4.7 Determination of color variations

Many applications require that the hydrophobic fabric treatment do not alter the color or other aesthetic properties of the fabrics [53]. Colorimetric tests were performed according to the CIEL*a*b system, using the portable Konica Minolta CM 2600d spectrophotometer with the small area view (SAV) of 3 mm, the 10° detector and the D65 primary source [56]. Color coordinates were measured according to the CIE 1976 parameters to quantify the colorimetric variations produced by the polymeric coatings on the cotton textiles. The overall color parameter, ΔE, represents the deviation from the original value due to the coating, as a cumulative effect of L*, a* and b* parameters and was calculated according to the formula:

$$\Delta E^*_{ab} = \sqrt{(\Delta L^*)^2 + (\Delta a^*)^2 + (\Delta b^*)^2}$$

where L* is the brightness vector on a gray scale from 0 (black) to 100 (white), a* is the red/green color component with values around zero (green being negative and red being positive), b* stands for the blue/yellow component (blue being negative and yellow positive).

2.4.8 Ageing in climatic chamber

The long term durability of the treated hydrophobic fabrics was further evaluated through ageing tests [57]. The treated and untreated fabrics were placed in a Memmert Climate chamber with three cold light fluorescent lamps (D65, 6500K) and two UV lamps (320-400 nm), at 20°C and 40% R.H. Samples underwent an accelerated ageing of 7.5 Mlxh (million lux hours), which is comparable to five times the average annual exposure found in museum illuminated environment [58]. After the ageing, colorimetric analysis was repeated, to assess the influence of the coatings on the aesthetical properties of the fabrics [59].

2.4.9 Washing/Laundry Resistance

To investigate the effect of laundry cycles on the hydrophobicity of the fabrics, we conducted experiments to simulate several washing cycles. Details of the procedure followed could be found in [60]. Fabric samples were laundered in water containing a commercial detergent (22 g/kg load) under stirring at 40 °C for 1 h. For each new wash cycle, a fresh amount of detergent was added which is not commonly reported in literature in order to ensure each cycle is done in the presence of surfactants. At the end of each cycle, the fabrics were rinsed with fresh deionized water and dried under ambient conditions for a period of 48 hours.

3. RESULTS AND DISCUSSION

3.1 Morphological characterization

The dense woven structure of the untreated fabric is clearly seen in the SEM image of **Fig. 2a.** Untreated fabric fibers showed a typical convoluted and wrinkle like structure [61] due to the longitudinal fibril structure [17]. The double layer formed by dip coating produces a very

smooth fiber surface morphology (**Fig. 2b**) and all the fibers are clearly visible with no coatings covering fiber bundles. Morphology of the cotton fabric dip coated with the PCU/aminosilicone emulsion (S3) appears very similar to the untreated texture indicating that the treatment does not form any coating but rather impregnates the fabric texture as seen in **Fig. 2c**. The inset SEM image of **Fig. 2c** at higher magnification demonstrates convoluted fiber structure similar to the untreated fibers with open pores. In contrast, a double layer coating approach (PCU and aminosilicone) using spray application (S4 sample in **Fig.2d**) produced a type of coating on the fabric as many individual fibers were not easily distinguishable from each other. The inter-fiber spaces were also partially filled with the polymers as seen in **Fig. 2d**. The cellulosic fiber morphology was smoothed out by the polymer coating. Interestingly, S5, the cotton fabric spray coated with PCU/aminosilicone emulsion (**Fig. 2e**) did not create a coating over the fabric and no closure of inter-fiber spaces due to polymers was observed. However, as the inset in **Fig. 2e** shows, spraying related micro-bumps on the fiber surfaces formed after application.

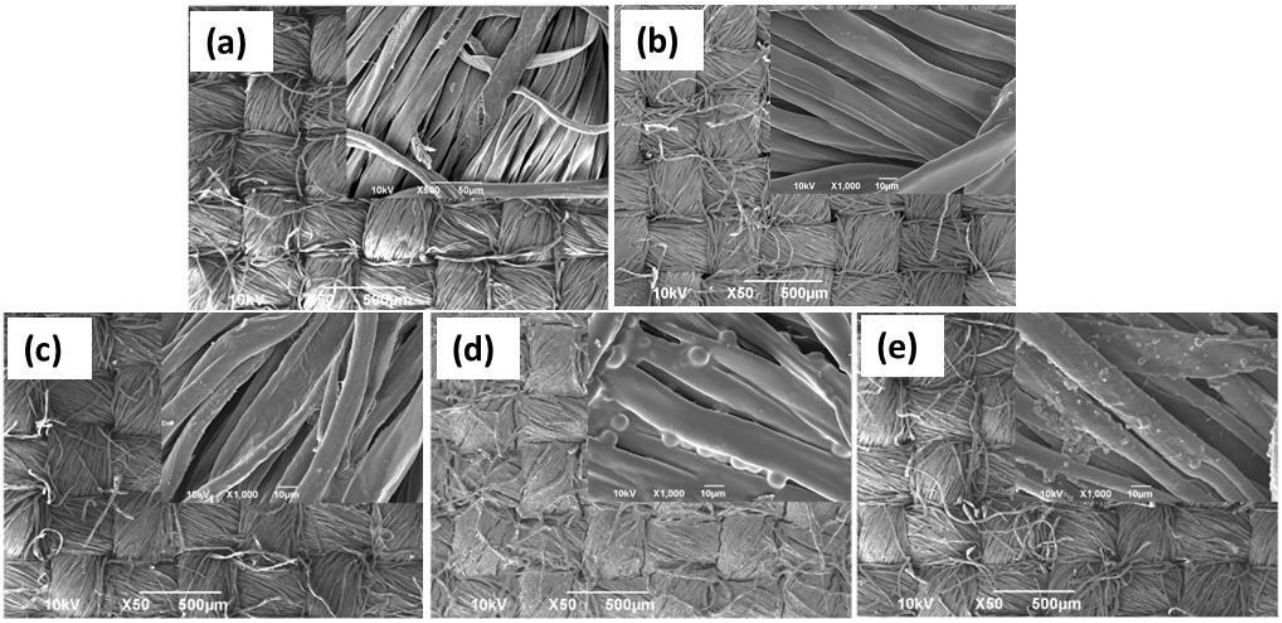

Figure 2. SEM images of (a) S1 untreated sample, (b) S2, (c) S3, (d) S4 and (d) S5. Inset SEM images show the surface morphology of corresponding fabrics at higher magnifications.

In general, spray coated fabrics showed rougher microscale features on the fibers' surface with respect to the fabrics treated with dip coating. This spray induced micro-roughness can be ascribed to the solvent evaporation during the flight of the atomized droplets toward the substrate

[62] and freezing of polymer solution droplets over the surfaces into microscale spherical structures [4].

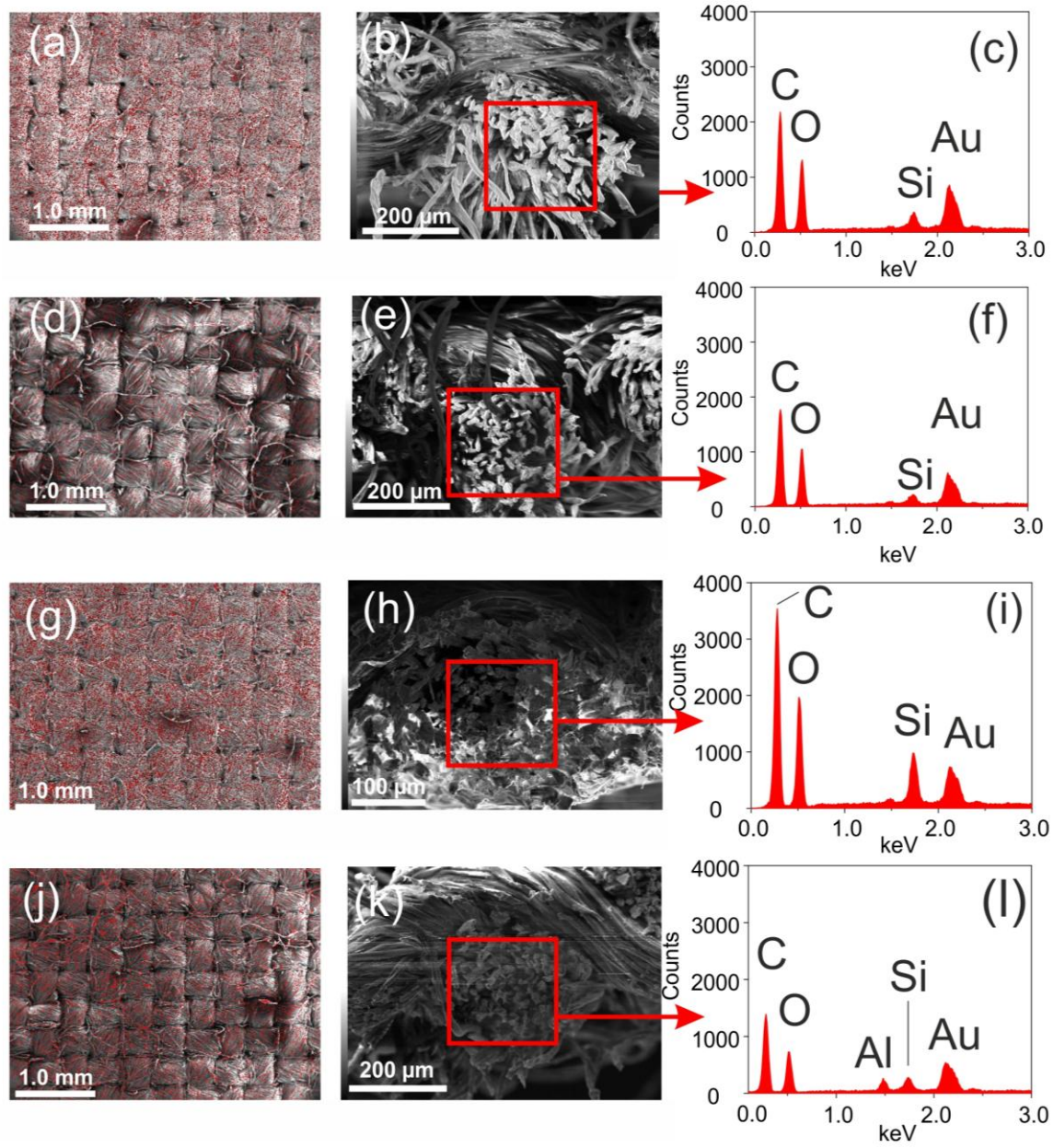

Figure 3. EDX analysis of treated cotton fabrics. Silicon mapping (in red color) of top surface, cross section of fabrics and relative EDX cross section spectra of (a-c) S2, (d-f) S3, (g-i) S4 and (j-l) S5. Silicon mapping has been indicated in red color.

Energy-dispersive X-ray spectroscopy (EDX) analyses of the treated fabrics were also performed (both surface and bulk cross section) in order to investigate the chemical homogeneity

of the treatments. Particularly, elemental Si dispersion was investigated (red points in **Fig. 3**). Indeed, the elemental silicon maps on the top surface demonstrates the degree of homogeneity of the formulations both for emulsion dip-coating (see **Fig. 3a** for S2 and **Fig. 3d** for S3), and emulsion spray coating (see **Fig. 3g** for S4 and **Fig. 3j** for S5). As mentioned, elemental spectra obtained from the cross sectional cuts were also performed in order to verify the penetration of the aminosilicone polymer. Spectra of all fabrics including the untreated ones demonstrate two distinct peaks at 0.277 keV and 0.525 keV for atomic carbon and oxygen, respectively [63]. Whereas, PCU/aminosilicone emulsion-treated cotton fabrics display an additional peak at 1.740 keV corresponding to atomic silicon [64], as shown in **Figs. 3 (c), (f), (i)** and **(j)**. Note that the presence of gold atoms in EDX spectra at 2.120 keV is due to the sputtering performed to enhance the conductivity of the substrate, while the presence of aluminum atoms at 1.486 keV is due to the aluminum stub on which samples were placed. Penetration of the PCU/aminosilicone emulsion into the fabric was achieved both by dip (**Figs. 3c** and **3f**) and spray coating (**Figs. 3i** and **3l**). This method of analysis cannot indicate which process (spray or dip) ensures better fabric penetration but it is useful as a qualitative indicator of treatment efficiency. Impregnation of aminosilicone into the fabric was also possible even if sequential treatment was performed as seen in **Fig. 3c** for S2, indicating that the PCU treatment does not block impregnation of the softener into the fabric bulk. The EDX spectra (obtained from the cross section) can be used to estimate the elemental distribution within each cross section and calculations yield 57% C, 36%O and 7%Si distribution in S2; 62%C, 34%O and 4% Si in S3; 54%C, 31%O and 16%Si in S4 and; 59%C, 32%O and 9%Si in S5 fabric. It appears that fabric S4 has the highest elemental silicone within the bulk textile but it must be noted that EDX spectra are sample depth dependent and this could create some errors in estimating real and reliable elemental compositions.

The sub-micron surface morphologies of the treated cotton fabric fibers were further characterized with AFM. The AFM analyses were performed on samples S1 and S5. 3D surface roughness profiles of the analyzed fabric fibers are shown in **Fig.4**. Both root mean square roughness (Sq) and average roughness (Sa) were calculated. The untreated cotton fiber has an intrinsic roughness at the nanoscale, which was not significantly modified by the spray treatment. Despite the process of atomization of the micro-emulsions during spray application increases the micro-roughness (**Fig. 2**), the overall nano-roughness has not been affected

significantly because of the self-leveling and skin forming properties of silicone [33], [65], [66], and smoothening property of PCU [67] polymers.

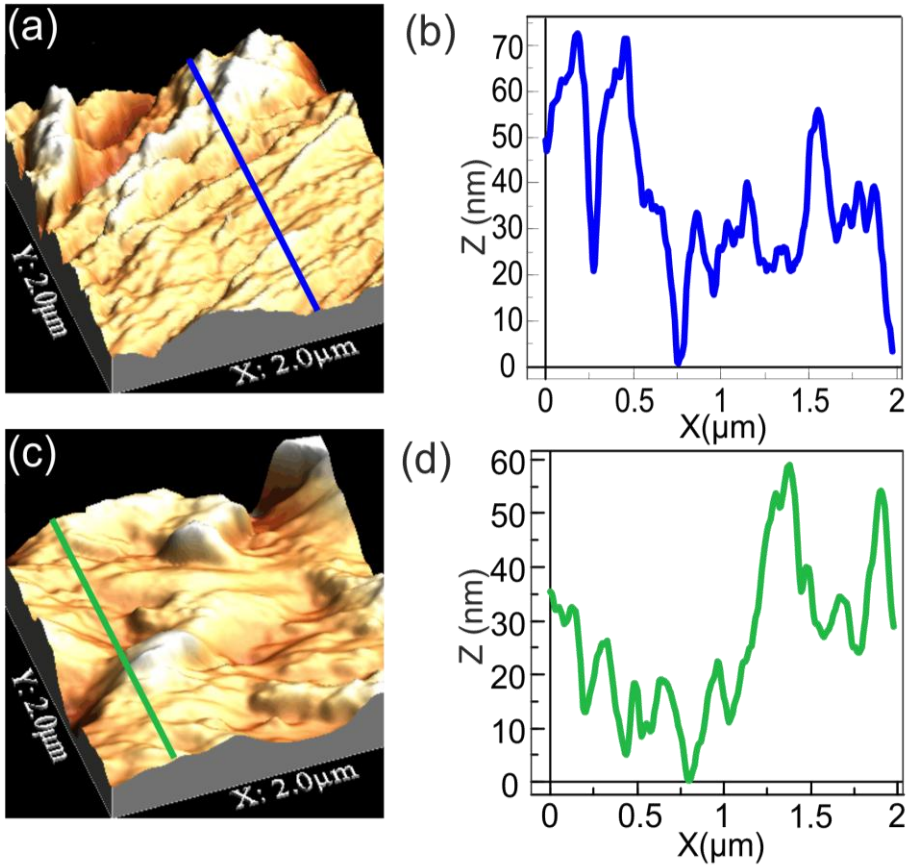

Figure 4. AFM topology analyses. (a) 3D topography reconstruction and (b) roughness profile of untreated cotton S1; (c) 3D topography reconstruction (d) and roughness profile of S5 cotton treated with micro-emulsion of PCU and aminosilicone by spray.

The average (Sq) roughness of the untreated cotton fiber was calculated to be 56.3 ± 19.4 nm [68]. Sq after treatment was approximately 64.3 ± 9.7 nm. Their corresponding average roughness (Sa) values were found to be 45.7 ± 14.4 nm and 47.2± 11.5 nm, respectively. This indicates that the submicro-scale roughness of the original untreated fibers as well as spraying induced microscale roughness (such as sample S5 in **Fig. 2d**) contributed to high hydrophobicity (WCA~ 145°) [17] and droplet mobility as will be demonstrated in the following sections.

3.2 Chemical characterization through attenuated total reflection-Fourier transform infrared (ATR-FTIR) spectroscopy.

The chemical characterization of the samples was carried out by ATR-FTIR spectroscopy, **Fig. 5**. **Figure 5a** shows the infrared spectra of pristine cotton, pure PCU, pure aminosilicone, and the S5 sample. Cotton showed the characteristic peaks of cellulose: OH stretching mode at 3297 cm^{-1}, CH stretching mode at 2883 cm^{-1}, adsorbed water at 1642 cm^{-1}, asymmetric C-C stretching mode at 1159 cm^{-1}, and C-O stretching mode at 1028 cm^{-1} [69]. On the other hand, PCU was characterized by urethane (N-H stretching mode at 3335 cm^{-1}, free and H-bonded C=O stretching modes at 1740 and 1707 cm^{-1}, N-H bending and C-N stretching modes at 1526 cm^{-1}, and C-O-C stretching mode at 1088 cm^{-1}), carbonate (the same free and H-bonded C=O stretching modes that for the urethanes groups, and the O-C-O stretching mode at 1242 cm^{-1}), and aliphatic (asymmetric and symmetric CH_2 stretching modes at 2922 and 2855 cm^{-1}, respectively) groups [70].

In the case of the aminosilicone, main peaks were CH_3 asymmetric and symmetric stretching modes at 2963 and 2905 cm^{-1}, respectively, $Si(CH_3)$ symmetric bending at 1258 cm^{-1}, Si-O-Si symmetric and asymmetric at 1074 and 1007 cm^{-1}, respectively, and CH_3 rocking at 783 cm^{-1}. It is expected that one would also detect peaks at 1731 and 1673 cm^{-1}, corresponding to -NH and $-NH_2$ vibration bands**.** The inability to detect these peaks is attributed to the fact that the molar content of the amino/amine functional groups is quite minute (~nano-molar) compared to the silicone polymer chain [71], [72] or even if they are detected in the pure silicone compound they disappear upon reacting with hydroxyl groups on fiber surfaces forming trace amounts of ammonia gas [73].

The infrared spectrum of the cotton spray coated with the blend of PCU and aminosilicone showed the bands of all three components. Two shifts in the O-H/N-H stretching and methylene rocking spectral regions were observed. **Figure 5b** compares the O-H/N-H stretching modes of cotton and coated cotton. The difference between the two spectra (coated cotton spectrum minus the cotton one) highlighted the presence of a band at ~3225 cm^{-1}. This is a typical value for N-H and O-H that strongly interact by H-bonds [74] indicating that hydroxyl groups of cotton and urethane and carbonate groups of PCU can interact through this kind of secondary bonds. In addition, a shift of ~13 cm^{-1} between the methyl rocking mode of silicone in pure silicone and the silicone together cotton and PCU was observed, **Figure 5c**. This phenomenon has been previously reported for cured PDMS in presence of different

polysaccharides or polysaccharide-rich materials, such as starch, cellulose, ethyl cellulose, red beetroot and cocoa shells wastes and explained by the formation of H-bonds between the O-H groups of the polysaccharide and the oxygen of the siloxane groups of the cross-linked PDMS [61], [75], [76], [77], [78].

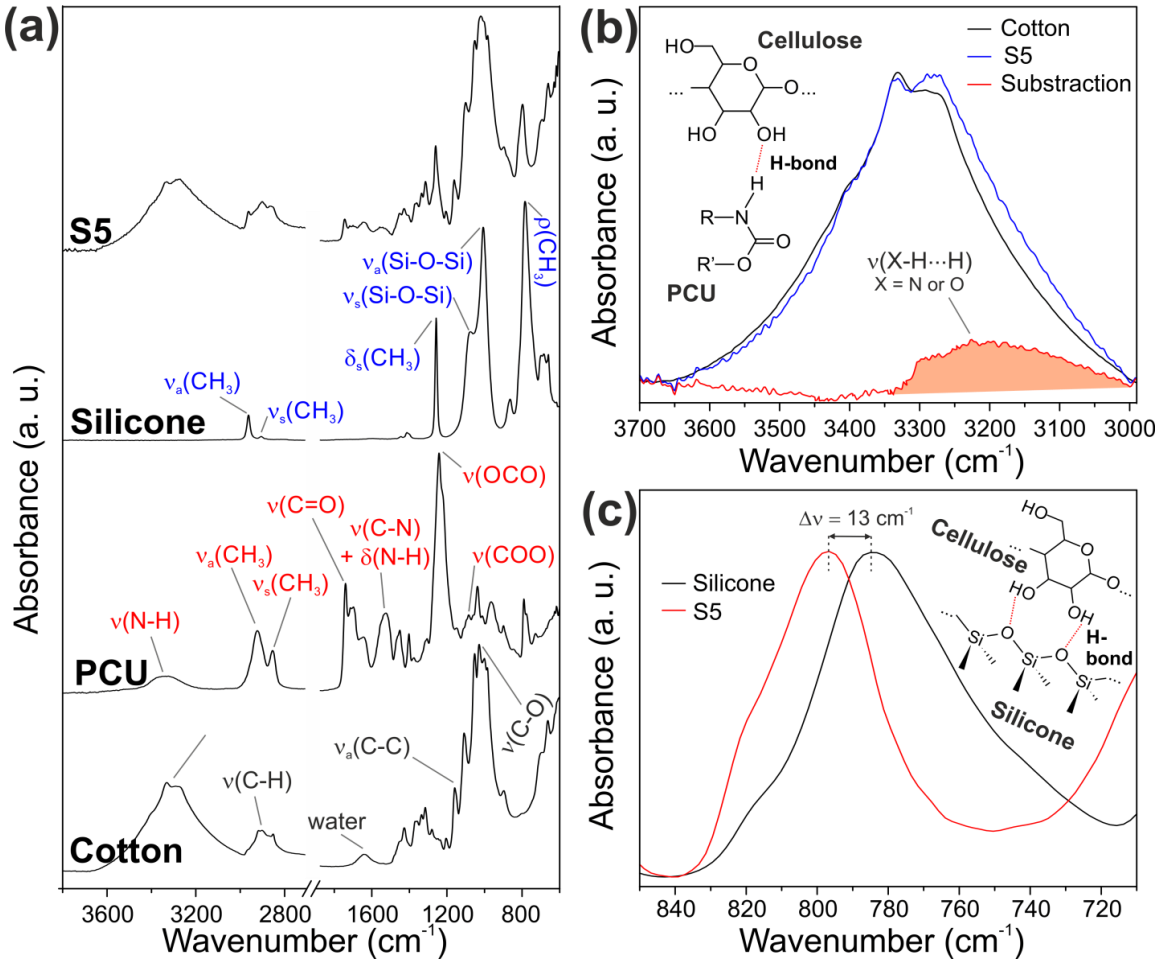

Figure 5. (a) ATR-FTIR spectra of cotton, PCU, aminosilicone, and S5 sample in the 3800-600 cm^{-1} region. The main assignments for cotton (black), PCU (red), and aminosilicone (blue) are included. (b) OH stretching band of cotton and cotton coated with the PCU-aminosilicone blend. The differences are highlighted with the subtraction of the two spectra. The possible interaction between cellulose and PCU by H-bonds is included. (c) CH_3 rocking band of aminosilicone and cotton coated with the PCU-aminosilicone micro-emulsion. The difference between the maxima of both peaks and the interaction between cellulose and aminosilicone by H-bonds are included.

Based on this analysis, it is highly probable that hydrogen bonding interactions exist between cellulose OH groups and amine groups of the silicone fluid, cellulose OH groups and

the OH groups of the aliphatic polycarbonate polyurethane chains and between amine groups of the silicone fluid and the OH groups of the polyurethane. These chemical interactions are shown in **Scheme 1** below.

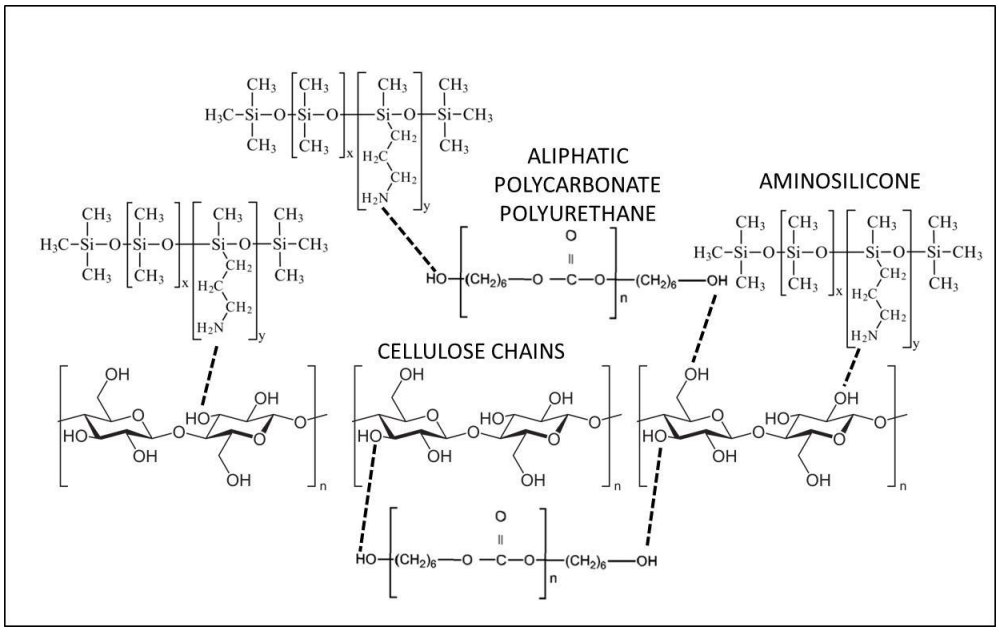

Scheme 1. Schematic representation of potential hydrogen bonding interaction among cotton surface, aliphatic polycarbonate polyurethane and aminosilicone fluid.

3.3 Wettability and surface energy

Surface wettability of the prepared cotton fabrics was analyzed by static and dynamic water contact angle measurements. For this, 5 µL water droplets were deposited on the surface of the fabrics and 10 different WCAs were measured on different locations of each fabric. Pristine cotton fibers are highly hygroscopic in nature and can absorb a significant amount of water on contact [12], [79]. The current measurement setup was unable to measure the water contact angle on untreated cotton fabric as the deposited water droplet immediately sank into the fabric. However, the cotton fabrics treated with different polymer formulations maintained water droplets in spherical shapes on their surface. WCAs for corresponding treated cotton fabrics are tabulated in **Figure 6a**. Note that all treatments conferred a good degree of hydrophobicity to the fabric. Both double-layer and PCU/aminosilicone emulsion applications produced static water contact angles between 143° and 147°.

a)

static contact angle (°)	
S1	n.a
S2	147° ± 4°
S3	145° ± 3°
S4	143° ± 2°
S5	145° ± 3°

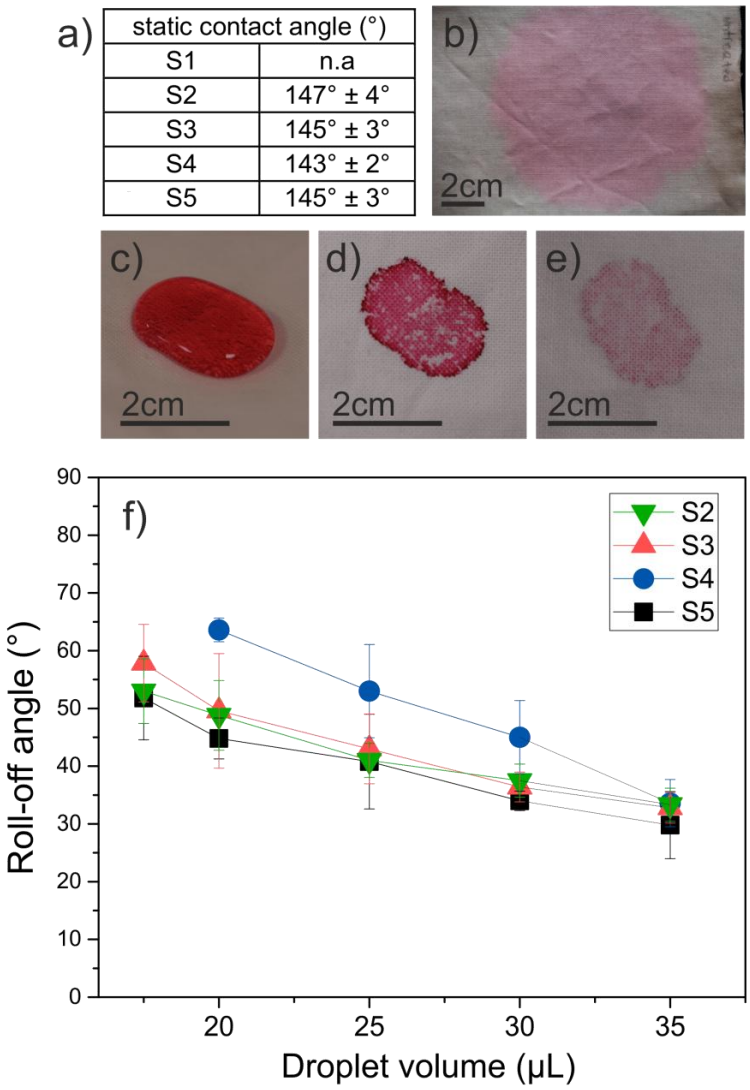

Figure 6. (a) Static water contact angles; (b) halo zone on S1 (untreated cotton); (c) colored water droplet on S5 (emulsion sprayed); (d) halo zone of S5; (e) halo zone back side of S5 when 1mL of colored water was deposited on samples; (f) water roll-off angle with increasing droplet volumes on samples S2 (double layer dip coating), S3 (emulsion dip coating), S4(double layer spray) and S5.

Larger volumes of colored water droplets (1 mL) were also deposited and their qualitative interaction with the fabric was monitored by observing color stain deposits after the droplets were removed or evaporated completely after some time. This also allowed potential monitoring of long-term droplet spreading during its evaporation. **Figure 6b** shows such a large stain on S1 due to the sudden sinking of a water droplet. On the other hand, all treated textiles (S2, S3, S4 and S5) showed stain marks which approximately corresponded to the initial contact

area of the 1 mL colored water droplet deposited on the textile (see **Figs. 6c-6e** of sample S5). The droplets evaporated in about 10 hours rather than spreading and sinking into the fabric under ambient conditions.

Considering that static WCAs appear to be very close for all the treatments, dynamic contact angle measurements have also been done to distinguish the hydrophobicity of each treatment from the other by using the concept of droplet mobility that indicates better hydrophobicity even if static WCAs appear to be similar *[80]*. Moreover, highly rough surfaces such as textile fabrics with protruding fibers or fiber fractions make it difficult to locate real droplet baseline during measurements of static WCA and can cause large error bars *[53]*, *[81]*. Therefore, the surface wettability was further studied by measuring roll-off or sliding angles of water droplets with varying droplet volume. For instance, given a droplet volume of 17.5µL, the water droplets started to roll-off the fabric surface at 52°, 53° and 58° tilt angles for S5, S2 and S3 fabrics, respectively (see **Figure 6f**). On the other hand, S4 sample was still sticky to 17.5 µL droplets when tilted at 90°. Except for fabric S4, all treatments demonstrated droplet mobility with lower roll of angles for larger volume droplets due to competition between gravitational and surface tension forces *[27]*. This self-cleaning effect was also achieved for sample S4 once droplet volume exceeded $\geq$ 30 µL that has been observed in textiles treated with various nanotechnology approaches as well *[82]*. The best performing treatment was determined to be S5, which demonstrated a water roll-off angle of 30° for 35 µL droplet volume. This is rather remarkable considering no fluorine chemistry, as well as nanoparticle induced surface texture modification, were used in the formulation. Moreover, the effect was achieved by a single spray application of the PCU/aminosilicone emulsion.

Note that treated fabrics without undergoing accelerated thermal annealing at 60^{o}C (drying and conditioning under ambient conditions for a month) performed identically to the samples shown in **Fig. 6**. Avoiding thermal annealing without sacrificing hydrophobic performance could be important if special fabrics, such as those used in Heritage preservation applications are to be targeted [79]. The surface free energy of the PCU/aminosilicone blend coatings applied on a glass slide was also estimated using different liquids of varying surface tensions.

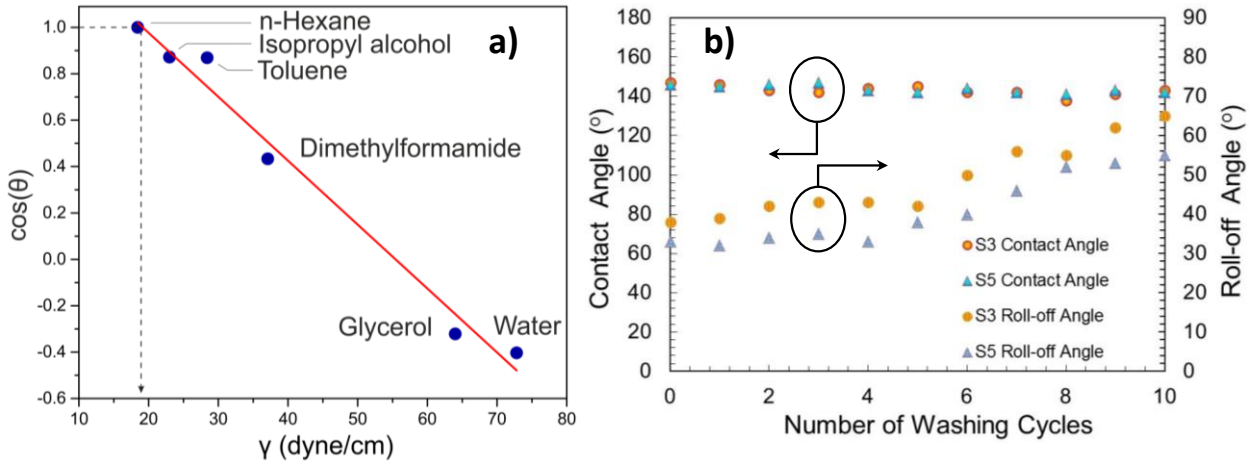

Figure 7. (a) Zisman plot for the flat film obtained from the micro-emulsion of PCU and aminosilicone. (b) Water contact angle and droplet (30 μL) roll–off angles for fabric samples S3 and S5 after as a function of number of laundry cycles.

The coating's critical surface energy was determined using a Zisman Plot. Zisman showed empirically that a plot of probing liquid cosine contact angle (cosθ) versus liquid surface tension (γ) is often linear [83]. Contact angles of six different liquids with well-known surface tensions were analyzed and plotted in (**Figure 7a**) over the PCU/aminosilicone polymeric surface. Linear regression of the experimental data gave the equation of the line: y=1.52784-0.02756x, with R^2=0.9782. At the point of the intersection with the value of cos(θ) = 1 a line was drawn perpendicular to the x-axis and a value of γ was read [48]. The surface energy of the coatings was estimated to be 19.5 dyne/cm, which is somewhat lower than pure silicone polymer surface energies reported in literature such as 22.8mN/m [84], 24.7 mN/m [85], 20.4 dyne/cm [86], and 24 mN/m at 20°C [87]. Combination of this low surface energy polymer blend with the fabric surface roughness and spray-induced micro-morphology is considered to be responsible for the droplet mobility on the treated fabrics. The changes in wetting properties of fabrics S3 and S5 after 10 laundry cycles are reported in **Figure 7b**. The static contact angles did not fluctuate significantly, however, droplet roll-off angles of both fabrics increased significantly after the 6th washing cycle. Fabric S5 demonstrated a lower roll-off contact angle than S3 at the end of the 10th laundry cycle. At this point, the deterioration of the wetting properties were not highly unfavorable but can be attributed to potential surfactant adsorption (laundry detergent) effects. No visible coating loss was noticed in the washing medium at the end of each washing cycle. Further characterization of the laundry aged fabrics will be conducted in a future work.

However, results in **Figure 7b** indicate that the treatment has a certain degree of durability against washing fastness.

3.4 Water vapor permeability

To evaluate the breathability of the treated cotton fabrics, water vapor permeability (WVP) was measured [9], [47], [76], [88]. The average WVP of the untreated cotton is calculated to be ~ $5.6 \cdot 10^{-3}$ g(m day Pa)$^{-1}$. This value corresponds to the permeability of the starting material, which is considered to be highly breathable. After hydrophobic treatments, all analyzed fabrics indicated WVP values that are very close to the original fabric as shown in

Table 2.

Table 2. Water vapor permeability (WVP of untreated and treated cotton. The average measurement uncertainty was within 0.2×10^{-3} g(m day Pa)$^{-1}$.

Sample	S1	S2	S3	S4	S5
WVP / g(m day Pa)$^{-1}$	5.6×10^{-3}	5.7×10^{-3}	5.3×10^{-3}	5.7×10^{-3}	5.7×10^{-3}

WVP could occur in different modes such that pores allow direct through transfer but also water molecules can diffuse through a polymer layer as well [89]. For fabrics, if the treatment does not fill up the inter-fibrillary spaces or pores (see **Fig. 2**), then the first mechanism occurs readily [35]. However, the PCU component of the blend, if one considers a treatment like a full coating, is known to promote vapor transport by the molecular mechanism of sorption-diffusion–desorption, where water vapor molecules are absorbed by the polymer, diffused across the bulk and fabric fiber, transferred to the other side, and finally released to the environment due to the hydrophilic moieties in polyurethanes [35].

3.5 Tensile strength and flexural rigidity

For the mechanical characterization of the fabrics, stress-strain tests were performed [51], [52], [55]. The textile construction with its yarn undulation generally yields a bilinear-like stress-strain response [52], which is also shown in **Figure 8a**; see also inset. The first slope corresponds to the stress in the single yarn, which increases under small strains and lengthens and tries to resist further stain induced deformation. The second slope corresponds to the irreversible

stretching after overcoming the preceding strain levels and individual fibers start to elongate within the woven network. In general, Young's or elastic modulus is calculated from the first slope of the stress-strain curves and they were reported in **Figure 8b** together with elongation at break values. Elastic modulus of all samples, except for S4 and to a certain extend S2 (double layer by dip or spray coating), were similar to the untreated textile. As seen in SEM analyses (**Fig. 2c**), the treatment applied as a double-layer filled the inter-fiber gaps potentially causing stiffer threads preventing them to slide over each other under stress.

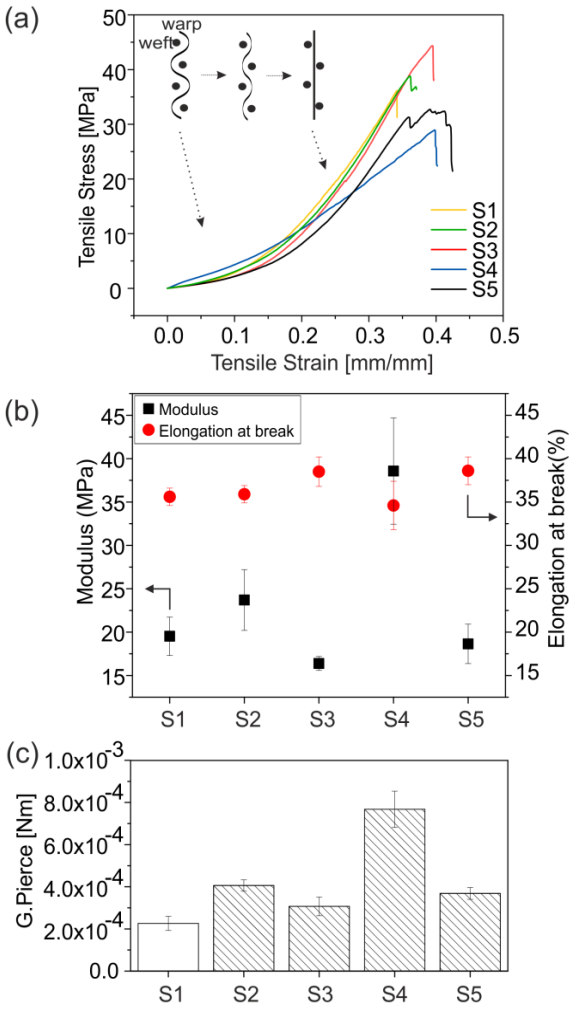

Figure 8. Mechanical tests. (a) stress-strain curve, (b) Modulus (MPa) and maximum percent elongation at break point of most promising treated samples, (c) stiffness calculated though G.Peirce cantilever test (see Table 1 for sample details).

On the other hand, both samples treated with the PCU/aminosilicone emulsion had moduli comparable to the untreated textile that is good for the sensational aspects of the fabric quality. It

is basically impossible to distinguish between these treated fabrics and untreated ones by touching them. Moreover, elongation at break remained unchanged for all the samples studied.

The bending stiffness of a textile is also an important mechanical feature that determines fabric drapability and handling. The Peirce cantilever test (ASTM D1388) was performed in order to determine multi-directional stiffness and to provide a more complete assessment of the anisotropic mechano-physical properties of the fabrics [54]. The length of a fabric bent under its own weight to a definite angle is related to its inherent stiffness. The longer the "bending length", the stiffer the fabric is. Results obtained through these cantilever tests are shown in **Figure 8c**. Stiffness of samples S3 and S5 was closer to the untreated fabric and stiffer fabrics formed after the double-layer treatment, confirming the results of stress-strain mechanical tests. Peirce cantilever test also qualitatively indicates good fabric flexibility since the stiffness measurement is obtained by bending the fabric.

3.6 Color variation

It is important that the hydrophobic textile treatments do not change or degrade the inherent color(s) of textiles. In fact, such treatments should maintain the original color unchanged or at least under the limiting value of 3 ΔE, so that the appearance of the fabric is not compromised. **Figure 9** shows the measured colorimetric variations due to different hydrophobic treatments. It is seen that color variations are much below 3 and even after simulated ageing corresponding to five years; ΔE values do not even exceed 2.

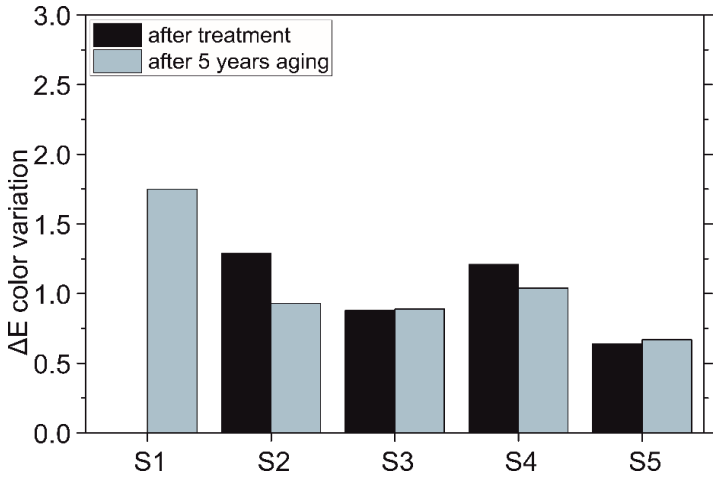

Figure 9. ΔE colorimetric values of samples after treatment (black) and after ageing (grey) with respect to untreated one.

The best performance was seen in S5 with a color variation of about 0.6 after application. Hence, all the treatments would be relevant and beneficial for the conservation of Heritage-related fabrics since the condition $\Delta E<3$ is not detectable by human eye. The untreated cotton textile had an overall ΔE of 1.8 after 5 years of accelerated ageing, and all treated samples had an overall ΔE between 0.9 and 1.8, after undergoing 7500000 lux·hours of UV-Vis radiation, comparable to five years of exposure in the National Gallery (UK). Hence, the coatings had a protective role with respect to UV-Vis radiation, which is probably due to the silicone component as silicones are known to be more resilient against UV-Vis than polyurethanes [56], [91].

4. CONCLUSIONS

Woven cotton fabrics were hydrophobized by transforming a functional silicone fluid commonly used as a fabric softener into an emulsion with an aqueous dispersion of polycarbonate diol polyurethane using isopropyl alcohol as co-solvent. The emulsions were stable with droplet diameters of approximately 1.5 μm. Polycarbonate polyurethane was used for its hydrolytic stability and low water absorption levels. Hydrophobic cotton fabrics were produced by simple immersion or spray coating approaches. Measured static water contact angles exceeded 143^{o} with droplet shedding angles of less than 50^{o} depending on the droplet volume. The estimated surface energy of the polymer blend was found to be 19.5 dyne/cm, slightly more hydrophobic compared to polydimethylsiloxane. After treatment, vapor permeability levels of 5.6 mg $(m\ day\ Pa)^{-1}$ was measured, similar to untreated fabrics. No nanoparticles were used in the formulations that are generally needed for creating texture on textiles. Accelerated ageing tests corresponding to 5 years with 7.5×10^{6} lux·hours exposure yielded no yellowing or ageing of the fabrics with the overall color parameter $\Delta E<2.0$. This simple textile hydrophobization method can be easily scaled out of the laboratory and can be potentially used for the treatment of Heritage valuable fabrics; but also for commercial cotton-based textiles.

REFERENCES

[1] J. Wang, F. Han, B. Liang, G. Geng, Hydrothermal fabrication of robustly superhydrophobic cotton fibers for efficient separation of oil/water mixtures and oil-in-water emulsions, Journal of Industrial and Engineering Chemistry. 54 (2017) 174–183. doi:10.1016/j.jiec.2017.05.031.

[2] X. Zhou, Z. Zhang, X. Xu, F. Guo, X. Zhu, X. Men, B. Ge, Robust and Durable Superhydrophobic Cotton Fabrics for Oil/Water Separation, ACS Applied Materials & Interfaces. 5 (2013) 7208–7214. doi:10.1021/am4015346.

[3] J.H. Lee, D.H. Kim, Y.D. Kim, High-performance, recyclable and superhydrophobic oil absorbents consisting of cotton with a polydimethylsiloxane shell, Journal of Industrial and Engineering Chemistry. 35 (2016) 140–145. doi:10.1016/j.jiec.2015.12.025.

[4] K. Sasaki, M. Tenjimbayashi, K. Manabe, S. Shiratori, Asymmetric Superhydrophobic/Superhydrophilic Cotton Fabrics Designed by Spraying Polymer and Nanoparticles, ACS Applied Materials & Interfaces. 8 (2016) 651–659. doi:10.1021/acsami.5b09782.

[5] J.Y. Huang, S.H. Li, M.Z. Ge, L.N. Wang, T.L. Xing, G.Q. Chen, X.F. Liu, S.S. Al-Deyab, K.Q. Zhang, T. Chen, Y.K. Lai, Robust superhydrophobic TiO@fabrics for UV shielding, self-cleaning and oil–water separation, Journal of Materials Chemistry A. 3 (2015) 2825–2832. doi:10.1039/C4TA05332J.

[6] Y. Liu, J.H. Xin, C.-H. Choi, Cotton Fabrics with Single-Faced Superhydrophobicity, Langmuir. 28 (2012) 17426–17434. doi:10.1021/la303714h.

[7] Q. Liu, J. Huang, J. Zhang, Y. Hong, Y. Wan, Q. Wang, M. Gong, Z. Wu, C.F. Guo, Thermal, Waterproof, Breathable, and Antibacterial Cloth with a Nanoporous Structure, ACS Appl. Mater. Interfaces. 10 (2018) 2026–2032. doi:10.1021/acsami.7b16422.

[8] K. Jeyasubramanian, G.S. Hikku, A.V.M. Preethi, V.S. Benitha, N. Selvakumar, Fabrication of water repellent cotton fabric by coating nano particle impregnated hydrophobic additives and its characterization, Journal of Industrial and Engineering Chemistry. 37 (2016) 180–189. doi:10.1016/j.jiec.2016.03.023.

[9] A. Mukhopadhyay, Vinay Kumar Midha, A Review on Designing the Waterproof Breathable Fabrics Part I: Fundamental Principles and Designing Aspects of Breathable Fabrics, Journal of Industrial Textiles. 37 (2008) 225–262. doi:10.1177/1528083707082164.

[10] S. Shahidi, J. Wiener, Antibacterial Agents in Textile Industry, in: V. Bobbarala (Ed.), Antimicrobial Agents, InTech, 2012: pp. 387–406. doi:10.5772/46246.

[11] D. Aslanidou, I. Karapanagiotis, C. Panayiotou, Superhydrophobic, superoleophobic coatings for the protection of silk textiles, Progress in Organic Coatings. 97 (2016) 44–52. doi:10.1016/j.porgcoat.2016.03.013.

[12] G. Mazzon, I. Zanocco, M. Zahid, I. Bayer, A. Athanassiou, L. Falchi, E. Balliana, E. Zendri, Nanostructured coatings for the protection of textiles and paper, Ge-Conservación/Conservação. (2017) 180–188.

[13] H. Zhang, R.N. Lamb, Superhydrophobic treatment for textiles via engineering nanotextured silica/polysiloxane hybrid material onto fibres, Surface Engineering. 25 (2009) 21–24. doi:10.1179/174329408X271390.

[14] M.A. Shirgholami, M. Shateri Khalil-Abad, R. Khajavi, M.E. Yazdanshenas, Fabrication of superhydrophobic polymethylsilsesquioxane nanostructures on cotton textiles by a solution–immersion process, Journal of Colloid and Interface Science. 359 (2011) 530–535. doi:10.1016/j.jcis.2011.04.031.
[15] F. Liu, M. Ma, D. Zang, Z. Gao, C. Wang, Fabrication of superhydrophobic/superoleophilic cotton for application in the field of water/oil separation, Carbohydrate Polymers. 103 (2014) 480–487. doi:10.1016/j.carbpol.2013.12.022.
[16] M. Zhang, S. Wang, C. Wang, J. Li, A facile method to fabricate superhydrophobic cotton fabrics, Applied Surface Science. 261 (2012) 561–566. doi:10.1016/j.apsusc.2012.08.055.
[17] C.-H. Xue, S.-T. Jia, J. Zhang, L.-Q. Tian, Superhydrophobic surfaces on cotton textiles by complex coating of silica nanoparticles and hydrophobization, Thin Solid Films. 517 (2009) 4593–4598. doi:10.1016/j.tsf.2009.03.185.
[18] S. Qiang, K. Chen, Y. Yin, C. Wang, Robust UV-cured superhydrophobic cotton fabric surfaces with self-healing ability, Materials & Design. 116 (2017) 395–402. doi:10.1016/j.matdes.2016.11.099.
[19] H. Liu, J. Huang, F. Li, Z. Chen, K.-Q. Zhang, S.S. Al-Deyab, Y. Lai, Multifunctional superamphiphobic fabrics with asymmetric wettability for one-way fluid transport and templated patterning, Cellulose. 24 (2017) 1129–1141. doi:10.1007/s10570-016-1177-6.
[20] M.-J. Oh, S.-Y. Lee, K.-H. Paik, Preparation of hydrophobic self-assembled monolayers on paper surface with silanes, Journal of Industrial and Engineering Chemistry. 17 (2011) 149–153. doi:10.1016/j.jiec.2010.12.014.
[21] D.A. Ellis, S.A. Mabury, J.W. Martin, D.C.G. Muir, Thermolysis of Fluoropolymers as a potential source of halogenated organic acids in the environment, Nature. 412 (2001) 321–324.
[22] K. Steenland, C. Jin, J. MacNeil, C. Lally, A. Ducatman, V. Vieira, T. Fletcher, Predictors of PFOA Levels in a Community Surrounding a Chemical Plant, Environ Health Perspect. 117 (2009) 1083–1088. doi:10.1289/ehp.0800294.
[23] S.H. Barmentlo, J.M. Stel, M. van Doorn, C. Eschauzier, P. de Voogt, M.H.S. Kraak, Acute and chronic toxicity of short chained perfluoroalkyl substances to Daphnia magna, Environmental Pollution. 198 (2015) 47–53. doi:10.1016/j.envpol.2014.12.025.
[24] B. Mahltig, H.B. Bottcher, Modified Silica Sol Coatings for Water-Repellent Textiles, Journal of Sol-Gel Science and Technology. 27 (2003) 43–52.
[25] M. Aymerich, A.I. Gómez-Varela, E. Álvarez, M.T. Flores-Arias, Study of Different Sol-Gel Coatings to Enhance the Lifetime of PDMS Devices: Evaluation of Their Biocompatibility, Materials. 9 (2016) 728. doi:10.3390/ma9090728.
[26] S. Nagappan, D.B. Lee, D.J. Seo, S.S. Park, C.-S. Ha, Superhydrophobic mesoporous material as a pH-sensitive organic dye adsorbent, Journal of Industrial and Engineering Chemistry. 22 (2015) 288–295. doi:10.1016/j.jiec.2014.07.022.
[27] H.F. Hoefnagels, D. Wu, G. de With, W. Ming, Biomimetic Superhydrophobic and Highly Oleophobic Cotton Textiles, Langmuir. 23 (2007) 13158–13163. doi:10.1021/la702174x.
[28] B. Liu, T. Tian, J. Yao, C. Huang, W. Tang, Z. Xiang, X. Xu, J. Min, Superhydrophobic organosilicon-based coating system by a novel ultravoilet-curable method, Nanomaterials and Nanotechnology. 7 (2017) 184798041770279. doi:10.1177/1847980417702795.
[29] C. Cao, M. Ge, J. Huang, S. Li, S. Deng, S. Zhang, Z. Chen, K. Zhang, S. Al-Deyab, Y. Lai, Robust fluorine-free superhydrophobic PDMS–ormosil@fabrics for highly effective

self-cleaning and efficient oil–water separation, Journal of Materials Chemistry A. 4 (2016) 12179–12187. doi:10.1039/C6TA04420D.
[30] C. Dong, Z. Lu, P. Zhu, L. Wang, F. Zhang, Synthesis and Application of a Novel Modified Polysiloxane Polymer with High Reaction Activity as Water Repellent Agent for Cotton Fabrics, Journal of Engineered Fibers and Fabrics. 10 (2015) 10.
[31] J. Monkiewicz, B. Standke, M. Horn, P. Jenkner, Triamino- and fluoroalkyl functional organosiloxanes, US 6,491,838 B1, 2002.
[32] J. Li, S. Zhong, Z. Chen, X. Yan, W. Li, L. Yi, Fabrication and properties of polysilsesquioxane-based trilayer core–shell structure latex coatings with fluorinated polyacrylate and silica nanocomposite as the shell layer, Journal of Coatings Technology and Research. 15 (2018) 1077–1088. doi:10.1007/s11998-018-0044-9.
[33] P. Somasundaran, S.C. Mehta, P. Purohit, Silicone emulsions, Advances in Colloid and Interface Science. 128–130 (2006) 103–109. doi:10.1016/j.cis.2006.11.023.
[34] C. Ji, F. Li, Z. Yun, Synthesis and properties of phenyl carboxyl polydimethylsiloxane for fabrics treatment, Journal of Applied Polymer Science. 135 (2018) 45866. doi:10.1002/app.45866.
[35] S. Mondal, J.L. Hu, Water vapor permeability of cotton fabrics coated with shape memory polyurethane, Carbohydrate Polymers. 67 (2007) 282–287. doi:10.1016/j.carbpol.2006.05.030.
[36] Q.B. Meng, S.-I. Lee, C. Nah, Y.-S. Lee, Preparation of waterborne polyurethanes using an amphiphilic diol for breathable waterproof textile coatings, Progress in Organic Coatings. 66 (2009) 382–386. doi:10.1016/j.porgcoat.2009.08.016.
[37] A.K. Sen, Coated Textiles : Principles and Applications, Second Edition, CRC Press, 2007. doi:10.1201/9781420053463.
[38] H.-J. Buschmann, E. Schollmeyer, Improved Adhesion of Polyurethane Coating to Polyester Fabrics due to the Surface Fixation of Calixarenes, Journal of Adhesion Science and Technology. 24 (2010) 113–121. doi:10.1163/016942409X12538865056114.
[39] U. Meier-Westhues, Polyurethanes: Coatings, Adhesives and Sealants, Vincentz Network GmbH & Co KG, 2007.
[40] M. Zuber, K.M. Zia, S. Tabassum, T. Jamil, S. Barkaat-ul-Hasin, M.K. Khosa, Preparation of rich handles soft cellulosic fabric using amino silicone based softener, part II: Colorfastness properties, International Journal of Biological Macromolecules. 49 (2011) 1–6. doi:10.1016/j.ijbiomac.2011.01.025.
[41] L. He, W. Li, D. Chen, D. Zhou, G. Lu, J. Yuan, Effects of amino silicone oil modification on properties of ramie fiber and ramie fiber/polypropylene composites, Materials & Design. 77 (2015) 142–148. doi:10.1016/j.matdes.2015.03.051.
[42] A.K. Roy Choudhury, 6 - Softening, in: A.K. Roy Choudhury (Ed.), Principles of Textile Finishing, Woodhead Publishing, 2017: pp. 109–148. doi:10.1016/B978-0-08-100646-7.00006-0.
[43] S.M. Cakić, M. Špírková, I.S. Ristić, J.K. B-Simendić, M. M-Cincović, R. Poręba, The waterborne polyurethane dispersions based on polycarbonate diol: Effect of ionic content, Materials Chemistry and Physics. 138 (2013) 277–285. doi:10.1016/j.matchemphys.2012.11.057.
[44] V. García-Pacios, V. Costa, M. Colera, J.M. Martín-Martínez, Waterborne polyurethane dispersions obtained with polycarbonate of hexanediol intended for use as coatings, Progress in Organic Coatings. 71 (2011) 136–146. doi:10.1016/j.porgcoat.2011.01.006.

[45] Z. Li, Y. Xing, J. Dai, Superhydrophobic surfaces prepared from water glass and non-fluorinated alkylsilane on cotton substrates, Applied Surface Science. 254 (2008) 2131–2135. doi:10.1016/j.apsusc.2007.08.083.
[46] N. Ahmad, S. Kamal, Z.A. Raza, T. Hussain, F. Anwar, Multi-response optimization in the development of oleo-hydrophobic cotton fabric using Taguchi based grey relational analysis, Applied Surface Science. 367 (2016) 370–381. doi:10.1016/j.apsusc.2016.01.165.
[47] G. Tedeschi, S. Guzman-Puyol, U.C. Paul, M.J. Barthel, L. Goldoni, G. Caputo, L. Ceseracciu, A. Athanassiou, J.A. Heredia-Guerrero, Thermoplastic cellulose acetate oleate films with high barrier properties and ductile behaviour, Chemical Engineering Journal. 348 (2018) 840–849. doi:10.1016/j.cej.2018.05.031.
[48] K.G. Kabza, J.E. Gestwicki, J.L. McGrath, Contact Angle Goniometry as a Tool for Surface Tension Measurements of Solids, Using Zisman Plot Method. A Physical Chemistry Experiment, Journal of Chemical Education. 77 (2000) 63. doi:10.1021/ed077p63.
[49] T.T.T. Ho, T. Zimmermann, S. Ohr, W.R. Caseri, Composites of Cationic Nanofibrillated Cellulose and Layered Silicates: Water Vapor Barrier and Mechanical Properties, ACS Applied Materials & Interfaces. 4 (2012) 4832–4840. doi:10.1021/am3011737.
[50] J. Wu, J. Li, Z. Wang, M. Yu, H. Jiang, L. Li, B. Zhang, Designing breathable superhydrophobic cotton fabrics, RSC Advances. 5 (2015) 27752–27758. doi:10.1039/C5RA01028D.
[51] E. de Bilbao, D. Soulat, G. Hivet, A. Gasser, Experimental Study of Bending Behaviour of Reinforcements, Experimental Mechanics. 50 (2010) 333–351. doi:10.1007/s11340-009-9234-9.
[52] A. Maziz, A. Concas, A. Khaldi, J. Stålhand, N.-K. Persson, E.W.H. Jager, Knitting and weaving artificial muscles, Science Advances. 3 (2017) e1600327. doi:10.1126/sciadv.1600327.
[53] J. Zimmermann, F.A. Reifler, G. Fortunato, L.-C. Gerhardt, S. Seeger, A Simple, One-Step Approach to Durable and Robust Superhydrophobic Textiles, Advanced Functional Materials. 18 (2008) 3662–3669. doi:10.1002/adfm.200800755.
[54] B. Goetzendorf-Grabowska, A. Karaszewska, V. Vlasenko, A. Arabuli, Bending Stiffness of Knitted Fabrics, Fibres & Textiles in Eastern Europe. 22 (2014) 43–50.
[55] N. Lammens, M. Kersemans, G. Luyckx, W. Van Paepegem, J. Degrieck, Improved accuracy in the determination of flexural rigidity of textile fabrics by the Peirce cantilever test (ASTM D1388), Textile Research Journal. 84 (2014) 1307–1314. doi:10.1177/0040517514523182.
[56] E. Cappelletto, E. Callone, R. Campostrini, F. Girardi, S. Maggini, C. della Volpe, S. Siboni, R. Di Maggio, Hydrophobic siloxane paper coatings: the effect of increasing methyl substitution, Journal of Sol-Gel Science and Technology. 62 (2012) 441–452. doi:10.1007/s10971-012-2747-1.
[57] A. Marchetti, S. Pilehvar, L. 't Hart, D. Leyva Pernia, O. Voet, W. Anaf, G. Nuyts, E. Otten, S. Demeyer, O. Schalm, K. De Wael, Indoor environmental quality index for conservation environments: The importance of including particulate matter, Building and Environment. 126 (2017) 132–146. doi:10.1016/j.buildenv.2017.09.022.
[58] R.L. Feller, Accelerated aging: photochemical and thermal aspects, Getty Conservation Institute, Marina del Rey, CA, 1994.

[59] T.T. Schaeffer, Effects of light on materials in collections: data on Photoflash and related sources, 2nd printing, Getty Conservation Institute, Los Angeles, 2001.
[60] P. Cataldi, L. Ceseracciu, A. Athanassiou, I.S. Bayer, Healable Cotton–Graphene Nanocomposite Conductor for Wearable Electronics, (2017). doi:10.1021/acsami.7b02326.
[61] M. Zahid, J.A. Heredia-Guerrero, A. Athanassiou, I.S. Bayer, Robust water repellent treatment for woven cotton fabrics with eco-friendly polymers, Chemical Engineering Journal. 319 (2017) 321–332. doi:10.1016/j.cej.2017.03.006.
[62] A. Steele, I. Bayer, E. Loth, Inherently Superoleophobic Nanocomposite Coatings by Spray Atomization, Nano Letters. 9 (2009) 501–505. doi:10.1021/nl8037272.
[63] Y.J. Yun, W.G. Hong, D.Y. Kim, H.J. Kim, Y. Jun, H.-K. Lee, E-textile gas sensors composed of molybdenum disulfide and reduced graphene oxide for high response and reliability, Sensors and Actuators B: Chemical. 248 (2017) 829–835. doi:10.1016/j.snb.2016.12.028.
[64] M.M. Sugii, F.A. de S. Ferreira, K.C. Müller, D.A.N.L. Lima, F.C. Groppo, H. Imasato, U.P. Rodrigues-Filho, F.H.B. Aguiar, Physical, chemical and antimicrobial evaluation of a composite material containing quaternary ammonium salt for braces cementation, Materials Science and Engineering: C. 73 (2017) 340–346. doi:10.1016/j.msec.2016.12.084.
[65] T. Zhu, S. Li, J. Huang, M. Mihailiasa, Y. Lai, Rational design of multi-layered superhydrophobic coating on cotton fabrics for UV shielding, self-cleaning and oil-water separation, Materials & Design. 134 (2017) 342–351. doi:10.1016/j.matdes.2017.08.071.
[66] C.M. Kim, H.B. Lee, J.U. Kim, G.M. Kim, Fabrication of poly (lactic-co-glycolic acid) microcontainers using solvent evaporation with polydimethylsiloxane stencil, Journal of Micromechanics and Microengineering. 27 (2017) 125018. doi:10.1088/1361-6439/aa9591.
[67] D. Khang, S.Y. Kim, P. Liu-Snyder, G.T.R. Palmore, S.M. Durbin, T.J. Webster, Enhanced fibronectin adsorption on carbon nanotube/poly(carbonate) urethane: Independent role of surface nano-roughness and associated surface energy, Biomaterials. 28 (2007) 4756–4768. doi:10.1016/j.biomaterials.2007.07.018.
[68] K. Vinisha Rani, B. Sarma, A. Sarma, Plasma treatment on cotton fabrics to enhance the adhesion of Reduced Graphene Oxide for electro-conductive properties, Diamond and Related Materials. 84 (2018) 77–85. doi:10.1016/j.diamond.2018.03.009.
[69] P. Garside, P. Wyeth, Identification of Cellulosic Fibres by FTIR Spectroscopy - Thread and Single Fibre Analysis by Attenuated Total Reflectance, Studies in Conservation. 48 (2003) 269–275. doi:10.1179/sic.2003.48.4.269.
[70] A. Szelest- Lewandowska, B. Masiulanis, M. Szymonowicz, S. Pielka, D. Paluch, Modified polycarbonate urethane: Synthesis, properties and biological investigation in vitro, Journal of Biomedical Materials Research Part A. 82A (2007) 509–520. doi:10.1002/jbm.a.31357.
[71] Y. Wei, C. Zheng, P. Chen, Q. Yu, T. Mao, J. Lin, L. Liu, Synthesis of multiblock linear polyether functional amino silicone softener and its modification of surface properties on cotton fabrics, Polymer Bulletin. 76 (2019) 447–467. doi:10.1007/s00289-018-2375-1.
[72] M.C. Gutiérrez, M. López-Mesas, M.T. Lacorte, J. Cegarra, Infrared analysis of the amino group content in functional aminopolydimethylsiloxanes, Fibers and Polymers. 10 (2009) 437–441. doi:10.1007/s12221-009-0437-6.
[73] S. Yang, H. Yu, Y. Chen, F. He, X. Li, K. Lu, The degradation pathway of aminosilicone polymer in aqueous microemulsion by Fenton process, Polymer Degradation and Stability. 98 (2013) 464–470. doi:10.1016/j.polymdegradstab.2012.06.032.

[74] L.J. Bellamy, The Infrared Spectra of Complex Molecules, Chapman and Hall, New York, 1975.
[75] L. Ceseracciu, J.A. Heredia-Guerrero, S. Dante, A. Athanassiou, I.S. Bayer, Robust and Biodegradable Elastomers Based on Corn Starch and Polydimethylsiloxane (PDMS), ACS Appl. Mater. Interfaces. 7 (2015) 3742–3753. doi:10.1021/am508515z.
[76] T.N. Tran, U. Paul, J.A. Heredia-Guerrero, I. Liakos, S. Marras, A. Scarpellini, F. Ayadi, A. Athanassiou, I.S. Bayer, Transparent and flexible amorphous cellulose-acrylic hybrids, Chemical Engineering Journal. 287 (2016) 196–204. doi:10.1016/j.cej.2015.10.114.
[77] J.A. Heredia-Guerrero, L. Ceseracciu, S. Guzman-Puyol, U.C. Paul, A. Alfaro-Pulido, C. Grande, L. Vezzulli, T. Bandiera, R. Bertorelli, D. Russo, A. Athanassiou, I.S. Bayer, Antimicrobial, antioxidant, and waterproof RTV silicone-ethyl cellulose composites containing clove essential oil, Carbohydrate Polymers. 192 (2018) 150–158. doi:10.1016/j.carbpol.2018.03.050.
[78] M. Zahid, E.L. Papadopoulou, G. Suarato, V.D. Binas, G. Kiriakidis, I. Gounaki, O. Moira, D. Venieri, I.S. Bayer, A. Athanassiou, Fabrication of Visible Light-Induced Antibacterial and Self-Cleaning Cotton Fabrics Using Manganese Doped TiO2 Nanoparticles, ACS Appl. Bio Mater. 1 (2018) 1154–1164. doi:10.1021/acsabm.8b00357.
[79] A. Timar-Balazsy, D. Eastop, Chemical Principles of Textile Conservation, Routledge, London, 1998.
[80] L. Gao, T.J. McCarthy, A Perfectly Hydrophobic Surface (θA/θR = 180°/180°), J. Am. Chem. Soc. 128 (2006) 9052–9053. doi:10.1021/ja062943n.
[81] L. Xu, W. Zhuang, B. Xu, Z. Cai, Fabrication of superhydrophobic cotton fabrics by silica hydrosol and hydrophobization, Applied Surface Science. 257 (2011) 5491–5498. doi:10.1016/j.apsusc.2010.12.116.
[82] S. Wang, K. Liu, X. Yao, L. Jiang, Bioinspired Surfaces with Superwettability: New Insight on Theory, Design, and Applications, Chemical Reviews. 115 (2015) 8230–8293. doi:10.1021/cr400083y.
[83] W.A. Zisman, F.M. Fowkes, Contact Angle, Wettability, and Adhesion, in: Relation of the Equilibrium Contact Angle to Liquid and Solid Constitution, ACS, 1964: pp. 1–51.
[84] T. Métivier, P. Cassagnau, Compatibilization of silicone/fluorosilicone blends by dynamic crosslinking and fumed silica addition, Polymer. 147 (2018) 20–29. doi:10.1016/j.polymer.2018.05.070.
[85] S.M. Mirabedini, M. Mohseni, Sh. PazokiFard, M. Esfandeh, Effect of TiO2 on the mechanical and adhesion properties of RTV silicone elastomer coatings, Colloids and Surfaces A: Physicochemical and Engineering Aspects. 317 (2008) 80–86. doi:10.1016/j.colsurfa.2007.09.044.
[86] R.-J. Roe, Surface Tension of Polymer Liquids, in: The Journal of Physical Chemistry, 1968: pp. 2013–2017.
[87] M.J. Owen, The Surface Activity of Silicones: A Short Review, Industrial & Engineering Chemistry Product Research and Development. 19 (1980) 97–103. doi:10.1021/i360073a023.
[88] A.H. Bedane, H. Xiao, M. Eić, Water vapor adsorption equilibria and mass transport in unmodified and modified cellulose fiber-based materials, Adsorption. 20 (2014) 863–874. doi:10.1007/s10450-014-9628-6.

[89] A.A. Badr, A. El-Nahrawy, Moisture properties of raised 3-thread fleece fabric knitted with different face and fleecy yarns, Alexandria Engineering Journal. 55 (2016) 2881–2892. doi:10.1016/j.aej.2016.06.021.
[90] R. Dastjerdi, M. Montazer, S. Shahsavan, A new method to stabilize nanoparticles on textile surfaces, Colloids and Surfaces A: Physicochemical and Engineering Aspects. 345 (2009) 202–210. doi:10.1016/j.colsurfa.2009.05.007.
[91] F. Pino, P. Fermo, M. La Russa, S. Ruffolo, V. Comite, J. Baghdachi, E. Pecchioni, F. Fratini, G. Cappelletti, Advanced mortar coatings for cultural heritage protection. Durability towards prolonged UV and outdoor exposure, Environ Sci Pollut Res. 24 (2017) 12608–12617. doi:10.1007/s11356-016-7611-3.